

ONLINE SUPERVISED ACOUSTIC SYSTEM IDENTIFICATION EXPLOITING PRELEARNED LOCAL AFFINE SUBSPACE MODELS

Thomas Haubner, Andreas Brendel and Walter Kellermann

Multimedia Communications and Signal Processing, Friedrich-Alexander-University Erlangen-Nürnberg,
Cauerstr. 7, D-91058 Erlangen, Germany, thomas.haubner@fau.de

ABSTRACT

In this paper we present a novel algorithm for improved block-online supervised acoustic system identification in adverse noise scenarios by exploiting prior knowledge about the space of Room Impulse Responses (RIRs). The method is based on the assumption that the variability of the unknown RIRs is controlled by only few physical parameters, describing, e.g., source position movements, and thus is confined to a low-dimensional manifold which is modelled by a union of affine subspaces. The offsets and bases of the affine subspaces are learned in advance from training data by unsupervised clustering followed by Principal Component Analysis. We suggest to denoise the parameter update of any supervised adaptive filter by projecting it onto an optimal affine subspace which is selected based on a novel computationally efficient approximation of the associated evidence. The proposed method significantly improves the system identification performance of state-of-the-art algorithms in adverse noise scenarios.

Index Terms— Online Supervised System Identification, Acoustic Echo Cancellation, Model Learning, Local Affine Subspace, Model Selection

1. INTRODUCTION

Online Supervised Acoustic System Identification (OSASI) is one of the classical tasks in acoustic signal processing with a multitude of applications [1, 2]. In this paper we consider linear convolutive Multiple-Input Multiple-Output (MIMO) applications with high-level interfering noise sources which are prone to non-robust OSASI performance. Such situations are typically encountered in hands-free acoustic human-machine interfaces which operate in, e.g., driving cars with open windows, or factories, and often involve negative Signal-to-Noise-Ratios (SNRs). MIMO OSASI is usually tackled by frequency-domain adaptive filter algorithms which take for its optimization the statistical properties of the excitation signals, e.g., non-stationarity, temporal and spatial correlation, into account [3, 4]. Noise and interference in the observations is often addressed by Variable Step Size Selection (VSSS) methods which use either binary or smooth adaptation control. Binary adaptation control, which in the context of Acoustic Echo Cancellation (AEC) is applied to cope with double-talk, stipulates halting the adaptation during periods of high interference levels [5, 6]. In contrast, smooth adaptation control continuously adjusts the step size in dependence of a noise estimate. A powerful model-based approach for smooth adaptation control, based on an online Maximum Likelihood (ML) algorithm,

was introduced in [7]. However, VSSS-based algorithms still result in limited system identification performance for applications with persistent low SNR.

Besides adaptation control, the exploitation of prior knowledge about the unknown system has proven to be beneficial for OSASI with high-level interfering noise [8, 9, 10]. This prior knowledge is usually extracted in advance from a training data set of Room Impulse Response (RIR) samples. The main assumption behind these approaches is the existence of a low-dimensional manifold that is embedded in the high-dimensional space of adaptive filter parameters for a given OSASI scenario. This can be motivated by the assumption that the variability of the unknown RIRs is controlled by only few physical parameters, describing, e.g., source position movements, temperature changes or movement of furniture [11, 12]. There is a variety of different approaches to model this manifold with the most prominent one assuming that the RIRs are confined to a single affine subspace which can be estimated, e.g., by Principal Component Analysis (PCA). In [8] this model has been employed by regularizing a Least-Squares (LS) cost function with the Mahalanobis distance based on the estimated RIR covariance matrix. The strong assumption of globally-correlated RIRs is however only rarely valid in practice, e.g., see [12]. Thus, [9] modifies it to a local PCA model, which can be motivated by the assumption of manifolds being locally Euclidean [13]. By the increased model flexibility, which results from employing several PCAs instead of a single one, [9] shows a performance improvement in an offline LS-based system identification task. Hereby, each PCA is associated with a specific source position and estimated from RIR samples which correspond to local source position movements. By employing several mutually exclusive local models, a model selection is required. As selection criterion [9] suggests the Frobenius norm of the difference of the a-priori-learned model covariance matrices and an estimated Finite Impulse Response (FIR) covariance matrix. The latter one is estimated from the solutions of several LS system identification problems with local source position variations. In [10] another offline LS approach for noise-robust system identification is introduced which represents the training data by a globally-nonlinear manifold model. As [9] and [10] rely on an affinity measure between a statistic of the adaptive filter estimate and the model parameters, they are susceptible to nonunique solutions to the system identification problems which result, e.g., from cross-correlated input signals [14, 15].

In this paper we introduce a general method which allows to include prior knowledge about the RIRs into any OSASI algorithm to enhance its performance in adverse noise scenarios. The method relies on the assumption that the RIRs can be modelled by a set of affine subspaces whose parameters are estimated by unsupervised clustering and PCA. We suggest to denoise the estimated FIR coefficient updates of any OSASI algorithm by projecting it onto an op-

This work was supported by the DFG under contract no <Ke890/10-2> within the Research Unit FOR2457 "Acoustic Sensor Networks".

timally selected affine subspace. Furthermore, we introduce a probabilistic approach for computationally-efficient online model selection by evidence maximization which is independent of the current FIR estimate of the OSASI algorithm.

2. SUPERVISED ADAPTIVE MIMO FILTERING

In this section we will define a signal model for MIMO OSASI. Hereby, it is assumed that there exists a linear functional relationship between the n th sample of the Q estimated output signals

$$\hat{\mathbf{y}}(n) = \hat{\mathbf{H}}^T(n)\mathbf{x}(n) \in \mathbb{R}^Q \quad (1)$$

and the most recent L samples of the P input signals

$$\mathbf{x}(n) = (\mathbf{x}_1^T(n), \dots, \mathbf{x}_P^T(n))^T \in \mathbb{R}^{PL}, \quad (2)$$

with

$$\mathbf{x}_p(n) = (x_p(n), \dots, x_p(n-L+1))^T \in \mathbb{R}^L. \quad (3)$$

The estimated transmission matrix at time instant n

$$\hat{\mathbf{H}}(n) = \begin{pmatrix} \hat{\mathbf{h}}_{11}(n) & \dots & \hat{\mathbf{h}}_{1Q}(n) \\ \vdots & \ddots & \vdots \\ \hat{\mathbf{h}}_{P1}(n) & \dots & \hat{\mathbf{h}}_{PQ}(n) \end{pmatrix} \in \mathbb{R}^{PL \times Q} \quad (4)$$

models FIR filters $\hat{\mathbf{h}}_{pq}(n)$ of length L between each input and each output signal. As most algorithms directly process blocks of observations, we introduce the block output matrix

$$\hat{\mathbf{Y}}(m) = (\hat{\mathbf{y}}(mL), \dots, \hat{\mathbf{y}}(mL-L+1)) \in \mathbb{R}^{Q \times L} \quad (5)$$

which captures L samples into one block indexed by m .

The estimation of the transmission matrix Eq. (4) represents an optimization problem in the high-dimensional parameter space \mathbb{R}^R of dimension $R = PLQ$ with elements $\tilde{\mathbf{h}}(n) = \text{vec}(\hat{\mathbf{H}}^T(n))$ and $\text{vec}(\cdot)$ being the vectorization operator [16]. Then, the generic parameter update for iterative OSASI algorithms reads:

$$\tilde{\mathbf{h}}(m) = \tilde{\mathbf{h}}(m-1) + \Delta\tilde{\mathbf{h}}(m) \quad (6)$$

with $\Delta\tilde{\mathbf{h}}(m)$ denoting the update term. Note that in the following the block-dependency m of the parameters $\tilde{\mathbf{h}}(m)$ is omitted if possible for notational convenience.

3. LOCAL AFFINE SUBSPACE MODELS

As discussed in Sec. 1, the latent FIR coefficient vectors often populate only a structured subset of the high-dimensional space \mathbb{R}^R of adaptive filter parameters [11], which leads to the assumption of a low-dimensional manifold that can be learned in advance from a set of G training data samples $\tilde{\mathbf{h}}_g$ with $g = 1, \dots, G$.

With the assumption of manifolds being locally Euclidean [13], the coefficient vector manifold can be approximated by patches of locally tangential hyperplanes \mathcal{M}_i as illustrated exemplarily in Fig. 1 for $R = 3$. Each tangential hyperplane \mathcal{M}_i describes a local approximation of the manifold. This motivates the idea of confining the FIR coefficient vectors $\tilde{\mathbf{h}}$ to a union

$$\mathcal{M}_{\text{loc}} = \mathcal{M}_1 \cup \dots \cup \mathcal{M}_I \quad (7)$$

of I affine subspaces $\mathcal{M}_i := \{\tilde{\mathbf{h}}_i + \mathbf{V}_i\boldsymbol{\beta}_i \mid \boldsymbol{\beta}_i \in \mathbb{R}^{D_i}\}$ of dimension D_i . Each subspace \mathcal{M}_i is defined by its offset $\tilde{\mathbf{h}}_i$ and its basis matrix

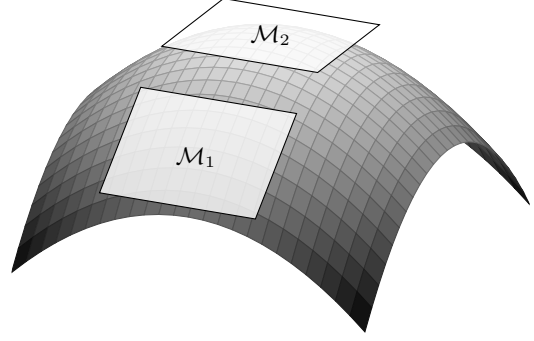


Fig. 1: Local tangential hyperplane approximation of the FIR coefficient vector manifold for $R = 3$.

$\mathbf{V}_i \in \mathbb{R}^{R \times D_i}$. While estimating the offset and the basis of a single global affine subspace, i.e., $I = 1$, by, e.g., PCA, is straightforward, it is not obvious how to learn the parameters of the local models. However, as each affine subspace \mathcal{M}_i denotes a local approximation of the manifold, its parameters can be estimated from the surrounding training data samples. Therefore we first assign each training data sample $\tilde{\mathbf{h}}_g$ to a specific cluster \mathcal{U}_i by introducing the indicator variable z_{gi}

$$z_{gi} := \begin{cases} 1 & \text{if } \tilde{\mathbf{h}}_g \in \mathcal{U}_i, \\ 0 & \text{if } \tilde{\mathbf{h}}_g \notin \mathcal{U}_i \end{cases} \quad (8)$$

and then use the clustered data for estimating the model parameters. The mean and covariance matrix of the respective RIR cluster \mathcal{U}_i can be estimated by

$$\bar{\mathbf{h}}_i = \frac{1}{G_i} \sum_{g=1}^G z_{gi} \tilde{\mathbf{h}}_g \quad (9)$$

$$\mathbf{C}_i = \frac{1}{G_i - 1} \sum_{g=1}^G z_{gi} [(\tilde{\mathbf{h}}_g - \bar{\mathbf{h}}_i)(\tilde{\mathbf{h}}_g - \bar{\mathbf{h}}_i)^T] \quad (10)$$

with $G_i = \sum_{g=1}^G z_{gi}$. A local basis matrix \mathbf{V}_i can be computed by, e.g., the eigenvectors \mathbf{u}_i corresponding to the largest eigenvalues d_i of the parameter covariance matrix \mathbf{C}_i . Note that one is by no means limited to PCA for extracting the model parameters and can resort to any other algorithm for estimating a linear representation [17]. Due to the broadband definition of the filter parameters in Eq. (4), the covariance matrix \mathbf{C}_i describes, in addition to the correlation of different taps of one FIR filter $\tilde{\mathbf{h}}_{pq}$, also the correlation between different FIR filters. Note that $I = 1$ denotes the special case of dimension reduction by a single PCA which assumes globally-correlated FIR coefficient vectors, i.e., strong correlation between all RIR samples used as training data. The local affine subspace model relaxes this assumption by requiring only a local correlation, i.e., only subsets of the RIR training data are assumed to be correlated.

In [9] it was assumed that the clusters represent local source position variations and the assignment of the samples was given by oracle knowledge. As this oracle knowledge cannot be assumed in general and the resulting assignment is by no means guaranteed to be optimum, we suggest to learn the assignment blindly from the data by unsupervised K-Means clustering [18] which employs a Euclidean affinity measure which can only be assumed to be meaningful in a local neighbourhood of the samples.

4. LOCAL PROJECTION-BASED UPDATE DENOISING

In the previous section we have introduced the union of I affine subspace models as a low-dimensional approximation of the parameter space of RIR coefficient vectors. Now we will describe how to exploit this knowledge for the general OSASI update of the form (6) to become more robust against noise. The proposed algorithm is inspired by the theory of manifold optimization, e.g., [19], in which the main idea is to exploit prior knowledge about the structure of the parameter space, e.g., matrix properties, by computing the steepest descent direction with respect to the metric defined by the manifold.

4.1. Model Selection

A powerful method for model selection is given by the evidence maximization framework [20, 21]. It suggests to employ the likelihood of each model

$$p(\mathbf{Y}(m)|\mathcal{M}_i) = \int p(\mathbf{Y}(m)|\tilde{\mathbf{h}}, \mathcal{M}_i)p(\tilde{\mathbf{h}}|\mathcal{M}_i)d\tilde{\mathbf{h}}, \quad (11)$$

given by the evidence of the observations, as selection criterion. By assuming i.i.d. observations $\mathbf{y}(n)$, the evidence of block m is defined by

$$p(\mathbf{Y}(m)|\mathcal{M}_i) := \prod_{n=mL-L+1}^{mL} p(\mathbf{y}(n)|\mathcal{M}_i). \quad (12)$$

Note that the assumption of i.i.d. observations is only a simplifying modelling assumption and its validity depends on the statistical properties of the excitation signal and the system. If we assume a linear Gaussian model for the likelihood [22]

$$p(\mathbf{y}(n)|\tilde{\mathbf{h}}, \mathcal{M}_i) = p(\mathbf{y}(n)|\tilde{\mathbf{h}}) = \mathcal{N}(\mathbf{y}(n)|\tilde{\mathbf{X}}^T(n)\tilde{\mathbf{h}}, \mathbf{L}) \quad (13)$$

which is independent of the model \mathcal{M}_i and further assume a Gaussian prior for each model \mathcal{M}_i

$$p(\tilde{\mathbf{h}}|\mathcal{M}_i) = \mathcal{N}(\tilde{\mathbf{h}}|\tilde{\mathbf{h}}_i, \mathbf{C}_i), \quad (14)$$

the sample-wise evidence is given by [20]

$$p(\mathbf{y}(n)|\mathcal{M}_i) = \mathcal{N}(\mathbf{y}(n)|\tilde{\mathbf{X}}^T(n)\tilde{\mathbf{h}}_i, \mathbf{R}_i(n)) \quad (15)$$

with covariance matrix

$$\mathbf{R}_i(n) = \mathbf{L} + \tilde{\mathbf{X}}^T(n)\mathbf{C}_i\tilde{\mathbf{X}}(n). \quad (16)$$

We introduced here the input signal matrix $\tilde{\mathbf{X}}^T(n) = \mathbf{x}^T(n) \otimes \mathbf{I}_Q \in \mathbb{R}^{Q \times R}$ with \otimes denoting the Kronecker product and $\mathbf{I}_Q \in \mathbb{R}^{Q \times Q}$ being the identity matrix, and the observation noise covariance matrix $\mathbf{L} \in \mathbb{R}^{Q \times Q}$. Instead of employing the logarithmic evidence $\log p(\mathbf{Y}(m)|\mathcal{M}_i)$ of block m as objective function for model selection, we suggest to use the recursive average evidence estimator

$$\hat{\mathcal{E}}_i(m) = \lambda \hat{\mathcal{E}}_i(m-1) + (1-\lambda) \log p(\mathbf{Y}(m)|\mathcal{M}_i) \quad (17)$$

to reflect the smooth trajectories on the manifolds caused by RIR changes. The recursive averaging factor $\lambda \in [0, 1]$ in Eq. (17) models an exponential weighting of temporally preceding observations and needs to be chosen according to the time-variance of the RIR. Finally, the optimum model index $i^*(m)$ at block index m is computed by

$$i^*(m) = \operatorname{argmax}_{i=1, \dots, I} \hat{\mathcal{E}}_i(m). \quad (18)$$

We will now aim at interpreting the logarithmic evidence

$$\log p(\mathbf{y}(n)|\mathcal{M}_i) \stackrel{c}{=} -\frac{1}{2} \left(\log \det \mathbf{R}_i(n) + \bar{\mathbf{e}}_i^T(n) \mathbf{R}_i^{-1}(n) \bar{\mathbf{e}}_i(n) \right) \quad (19)$$

of the observed sample $\mathbf{y}(n)$ given the model \mathcal{M}_i with the estimated average observation error

$$\bar{\mathbf{e}}_i(n) = \mathbf{y}(n) - \tilde{\mathbf{X}}^T(n)\tilde{\mathbf{h}}_i \quad (20)$$

and $\stackrel{c}{=}$ denoting equality up to a constant term. As expected for evidence-based model selection [20, 21], Eq. (19) consists of two terms which trade model complexity, described by $\log \det \mathbf{R}_i(n)$, against data fitting, described by $\bar{\mathbf{e}}_i^T(n) \mathbf{R}_i^{-1}(n) \bar{\mathbf{e}}_i(n)$. By additionally assuming uncorrelated observations $\mathbf{y}(n)$, the logarithmic evidence (19) reduces to a sum of channel-wise measures

$$\log p(\mathbf{y}(n)|\mathcal{M}_i) \stackrel{c}{=} -\frac{1}{2} \sum_{q=1}^Q \left(\log \det r_{iq}(n) + \frac{|\bar{e}_i(n)|^2}{r_{iq}(n)} \right). \quad (21)$$

The data-fitting term is given by the weighted sum of the squared average observation errors $\bar{e}_i(n)$ of model \mathcal{M}_i . As the diagonal terms of the covariance matrix (see Eq. (16)) $r_{iq}(n)$ denote an estimate of the observation power, we can interpret the data-fitting term as a sum of the channel-dependent instantaneous inverse Echo Return Loss Enhancement (ERLE) performance measures [23] which are well-known in AEC. Thus, the logarithmic evidence (19) can be seen as an extension of the data-fitting ERLE performance measure which additionally penalizes complex models.

4.2. Efficient Evidence Approximation

As the direct evaluation of the logarithmic evidence by Eq. (19) is computationally demanding, we will now introduce an efficient approximation based on the low-dimensionality assumption of the subspaces. Therefore, we insert the Eigenvalue Decomposition (EVD) of the prior covariance matrix $\mathbf{C}_i = \mathbf{U}_i \mathbf{D}_i \mathbf{U}_i^T$ of model \mathcal{M}_i into the second term of the evidence covariance matrix computation (16)

$$\tilde{\mathbf{X}}^T(n)\mathbf{C}_i\tilde{\mathbf{X}}(n) = \tilde{\mathbf{X}}^T(n)\mathbf{U}_i\mathbf{D}_i^{\frac{1}{2}}\mathbf{D}_i^{\frac{1}{2}}\mathbf{U}_i^T\tilde{\mathbf{X}}(n) \quad (22)$$

$$= \tilde{\mathbf{X}}^T(n)\tilde{\mathbf{U}}_i\tilde{\mathbf{U}}_i^T\tilde{\mathbf{X}}(n) \quad (23)$$

$$= \sum_{r=1}^R \tilde{\mathbf{y}}_{ir}(n)\tilde{\mathbf{y}}_{ir}^T(n), \quad (24)$$

which shows that it can be computed by a sum of outer products. The existence of the matrix square root is guaranteed, due to the symmetry and positive semi-definiteness of the covariance matrix. Each vector $\tilde{\mathbf{y}}_{ir}(n)$ of the sum is computed by a multiplication of the input signal matrix with a scaled eigenvector $\tilde{\mathbf{u}}_{ir} = \mathbf{u}_{ir}\sqrt{d_{ir}}$ of the prior covariance matrix \mathbf{C}_i . As each matrix-vector product $\tilde{\mathbf{y}}_{ir}(n) = \tilde{\mathbf{X}}^T(n)\tilde{\mathbf{u}}_{ir}$ corresponds to a linear convolution of the input signals with a scaled eigenvector, i.e., eigenfilter, it can be efficiently computed by an overlap-save block processing structure. The latter also holds for the computation of the estimated average observation $\tilde{\mathbf{X}}^T(n)\tilde{\mathbf{h}}_i$ (see Eq. (15)).

Furthermore, as we originally assumed the existence of a lower-dimensional subspace (see Sec. 3), the ordered eigenvalues d_{ir} with $r = 1, \dots, R$ of the covariance matrix \mathbf{C}_i are assumed to exhibit a pronounced decay of magnitude. Hence, it is reasonable to approximate Eq. (24) by the $K_i = D_i$ largest terms corresponding to the dominant eigenvalues. Note that often K_i can be chosen much

smaller compared to D_i , i.e., $K_i \ll D_i$, as the first K_i eigenfilters provide sufficient discrimination for model selection. This allows for computationally efficient low-rank evidence approximations.

4.3. Projection

As each sub model \mathcal{M}_i denotes an affine subspace of \mathbb{R}^R , the parameter vector $\tilde{\mathbf{h}}^{p_i}$ resulting from orthogonal projection onto \mathcal{M}_i reads (see, e.g., [24])

$$\tilde{\mathbf{h}}^{p_i} = \bar{\mathbf{h}}_i + \mathbf{P}_i \left(\tilde{\mathbf{h}} - \bar{\mathbf{h}}_i \right) \quad (25)$$

with the rank-deficient projection matrix

$$\mathbf{P}_i = \mathbf{V}_i (\mathbf{V}_i^T \mathbf{V}_i)^{-1} \mathbf{V}_i^T. \quad (26)$$

Note that the projection matrix \mathbf{P}_i depends only on the training data and can thus be computed a priori.

4.4. Algorithmic Description

Alg. 1 gives a detailed description of the proposed Local Projection-based Update Denoising (LPUD) for OSASI. For each block of observations, indexed by m , the evidence estimates of all models \mathcal{M}_i are updated by Eq. (17). Hereby, the evidence $p(\mathbf{Y}(m)|\mathcal{M}_i)$ of block m , given model \mathcal{M}_i , is efficiently computed by an overlap-save processing and the low-rank evidence approximation derived in Sec. 4.2. If the optimum model index $i^*(m)$ has changed relative to the previous block, the previous parameter estimate $\tilde{\mathbf{h}}(m-1)$ is projected onto the optimum affine subspace $\mathcal{M}_{i^*(m)}$ by Eq. (25). This ensures that the updated FIR estimate will be confined to \mathcal{M}_{loc} . Subsequently, the parameter update $\Delta\tilde{\mathbf{h}}(m)$ is computed by a suitable OSASI algorithm and projected onto the optimum affine subspace by multiplication with the projection matrix $\mathbf{P}_{i^*(m)}$ (see Eq. (26)). Finally, the projected update is used for optimizing the adaptive filter coefficient vector (see Eq. (6)).

Algorithm 1 OSASI by LPUD

```

for  $m = 1, \dots, M$  do
  Update evidences of all  $I$  models by Eq. (17)
  Compute optimum model  $\mathcal{M}_{i^*(m)}$  by Eq. (18)
  if  $i^*(m) \neq i^*(m-1)$  then
    Project  $\tilde{\mathbf{h}}(m-1)$  onto opt. aff. subspace by Eq. (25)
  end if
  Compute parameter update  $\Delta\tilde{\mathbf{h}}(m)$ 
  Project parameter update:  $\Delta\tilde{\mathbf{h}}(m) \leftarrow \mathbf{P}_{i^*(m)} \Delta\tilde{\mathbf{h}}(m)$ 
  Update FIR coefficients:  $\tilde{\mathbf{h}}(m) \leftarrow \tilde{\mathbf{h}}(m-1) + \Delta\tilde{\mathbf{h}}(m)$ 
end for

```

5. EXPERIMENTS

In this section we will evaluate the proposed LPUD algorithm in a simulated environment with respect to its performance in noisy scenarios. Therefore, we consider an acoustic system identification scenario with $Q = 2$ microphones of 10 cm spacing and a single source, i.e., $P = 1$, located on a sector of a sphere with a radius of 1.3 m, an azimuth angle range $\theta \in [30^\circ, 150^\circ]$ and an elevation angle range $\phi \in [-5^\circ, 50^\circ]$. All PQ RIRs \mathbf{h}_{pq} have been simulated according to the image method [25, 26] with maximum reflection order for a room of dimension $[6, 5, 3.5]$ m with a reverberation time

of $T_{60} = 0.3$ s, a sampling frequency of $f_s = 8$ kHz and an RIR length of $W = 4096$ samples. The observed microphone signals have been sampled from the Gaussian density $\mathbf{y}(n) \sim \mathcal{N}(\mathbf{d}(n), \mathbf{L})$ with $\mathbf{d}(n) = \mathbf{H}^T \mathbf{x}(n) \in \mathbb{R}^Q$ denoting the true source image at the microphones and \mathbf{H} being the acoustic transmission matrix which includes the true RIRs \mathbf{h}_{pq} analogously to Eq. (4). The noise covariance matrix \mathbf{L} is a scaled identity matrix with the scale factor determined by the SNR.

For assessing the performance of the proposed algorithm, we introduce the signal-dependent average ERLE measure

$$\text{ERLE} = \frac{1}{(N_2 - N_1 + 1)Q} \sum_{n=N_1}^{N_2} \sum_{q=1}^Q \left(\frac{d_q(n)^2}{(d_q(n) - \hat{y}_q(n))^2} \right) \quad (27)$$

and the signal-independent average system mismatch

$$\Upsilon = \frac{1}{(M_2 - M_1 + 1)} \sum_{m=M_1}^{M_2} \Upsilon(m) \quad (28)$$

which is computed by the temporal average of the block-dependent system mismatch

$$\Upsilon(m) = \frac{1}{PQ} \sum_{p,q=1}^{P,Q} \left(\frac{\|\mathbf{h}_{pq} - \hat{\mathbf{h}}_{pq}(m)\|_2^2}{\|\mathbf{h}_{pq}\|_2^2} \right). \quad (29)$$

Note that, as the adaptive filter length L is usually much smaller than the true filter length W of the physical system to be modelled, we only use the first L taps of \mathbf{h}_{pq} to obtain an estimate of the attainable system mismatch. The observed signal that is caused by the remaining $W - L$ taps of the true RIR acts as an error in the introduced signal model Eq. (1) and results in an upper bound for the signal-dependent ERLE measure. It corresponds to the excess error in statistically optimum filtering [1].

As pointed out in Sec. 4, the presented method is not tied to any specific OSASI algorithm. In this paper we employ, as a fast-converging state-of-the-art algorithm, the Generalized Frequency-Domain Adaptive Filter (GFDAF) [3] which represents a computationally efficient optimization of the well-known block-recursive least-squares cost function in the frequency domain. For Single-Input Single-Output OSASI applications the GFDAF is equivalent to the popular FDAF [1] with a recursive power spectral density (PSD) estimation and an additional data-dependent dynamical regularization. We use a filter length of $L = 1024$ and no block overlap, a constant step size of $\mu = 1$, a recursive PSD averaging factor of $\nu = 0.9$ and the dynamical regularization parameters $\delta_{\max} = \delta_0 = 1$. Note that for stationary noise and non-stationary excitation signals, e.g., speech, VSSS is still beneficial due to the time-varying SNR.

In the following we will evaluate the proposed LPUD algorithm against two baselines, i.e., the raw GFDAF and a Global Projection-based Update Denoising (GPUD). The GPUD algorithm is a special case of the LPUD with $I = 1$. The training data for learning the model consisted of $G = 5000$ RIRs which were simulated according to randomly drawn source positions. The global affine subspace dimension is set to $D_1 = 550$ which showed good overall performance. The LPUD algorithm consists of $I = 40$ clusters of identical local dimension $D_i = 50$. The cluster assignment was learned by the K-Means algorithm [18, 27]. Furthermore, the evidence of each model \mathcal{M}_i was approximated by the $K_i = 5$ most dominant eigenfilters (see Sec. 4.2).

Fig. 2 shows the block-dependent system mismatch $\Upsilon(m)$ of all algorithms for different types of input signals, i.e., stationary

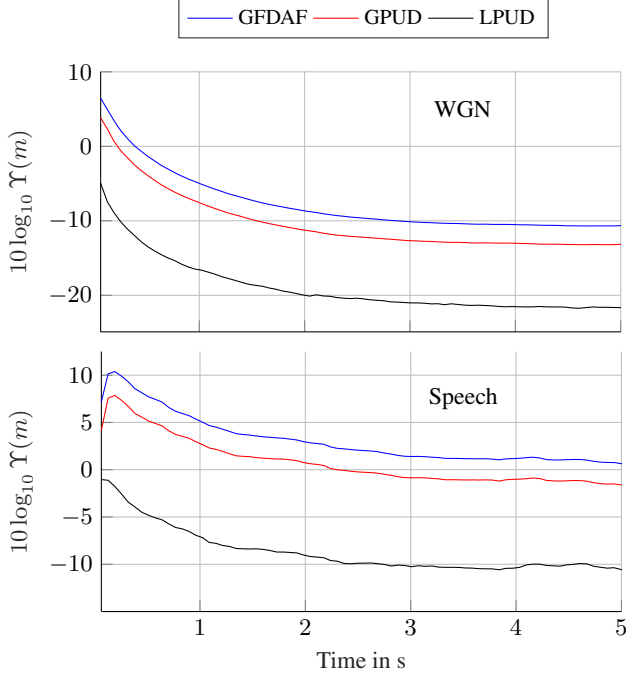


Fig. 2: Block-dependent system mismatch $\Upsilon(m)$ for a SNR of -5 dB in dependence of the excitation signal type.

White Gaussian Noise (WGN) and speech signals, and a SNR of -5 dB. For each type of input signal we have averaged $\Upsilon(m)$ over 50 independent Monte Carlo experiments which are defined by randomly drawing the source position and the source signals from the respective models. This limits the influence of a specific input signal and source position. As speech source signals we employed 20 different talkers reading out random concatenations of IEEE Harvard sentences [28]. As can be concluded from Fig. 2 all algorithms reach their steady-state estimate after approximately 3 s. While the steady-state performance of the GPUD improves only slightly in comparison to the GFDAF, the LPUD results in a significant improvement for both types of excitation signals. By comparing WGN to speech excitation, we observe that WGN shows consistently approximately 10 dB smaller system mismatch than speech for all algorithms. This reflects the well-known difference in convergence behaviour of adaptive filters caused by the nonstationarity and non-whiteness of speech signals [1, 3, 29]. While for this demanding scenario the state-of-the-art algorithm GFDAF is not capable of achieving a sufficient system identification performance anymore, the proposed LPUD achieves an average system mismatch of -10 dB after convergence. Additionally, by comparing the initial convergence phases of the algorithms, we observe an almost instantaneous gain of the LPUD which is caused by the projection on the estimated affine subspace. This results in superior system identification performance even during the early convergence phase, i.e., the first second.

In Fig. 3 we compare the respective algorithms for different SNR levels in terms of average ERLE and system mismatch. The results are averaged over 10 s of WGN excitation and 15 s of speech excitation and 50 independent Monte Carlo experiments. The respective limits of the sums in Eqs. (27) and (28), i.e., N_1, N_2, M_1, M_2 , are chosen to divide the signals into two parts of equal length. This allows to assess the Convergence Phase (CP), i.e., the first part, and the Steady-State (SS), i.e., the second part, independently. As can be concluded from Fig. 3 the proposed LPUD method significantly

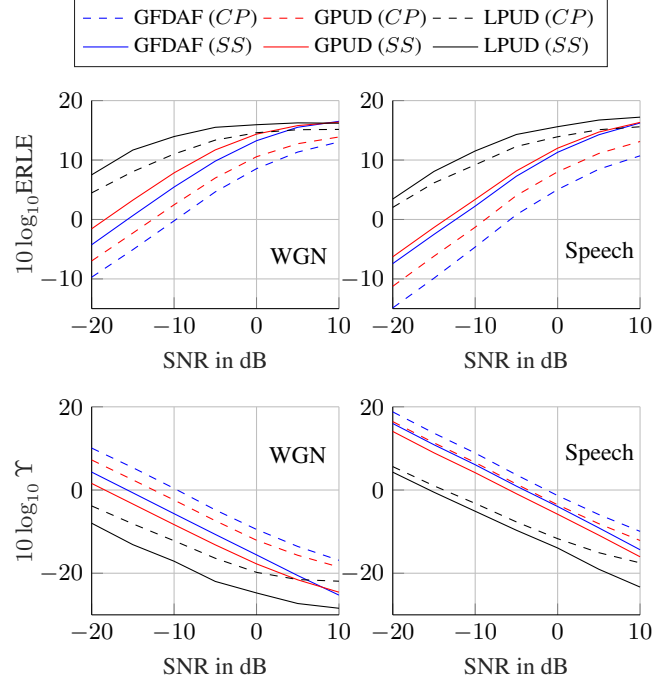


Fig. 3: Performance evaluation of the various algorithms in dependence of the SNR and the excitation signal type (CP: Convergence Phase, SS: Steady State).

outperforms the GFDAF for all SNR levels in terms of steady-state performance for both ERLE and system mismatch Υ . This suggests an efficient denoising of the update in low-SNR applications while still preserving a sufficient model flexibility for precise system identification in high-SNR scenarios. Additionally, by comparing the GPUD to the LPUD algorithm, one can observe the advantage of assuming only local linearity compared to the global linear approach which lacks the aforementioned trade-off opportunity. Finally, we observed that the optimum subspace dimensions D_i are strongly related to the respective SNR which would allow even higher performance improvements by choosing the signal-dependent optimum for each scenario.

6. SUMMARY AND OUTLOOK

In this paper we presented a novel method for improved OSASI in noisy environments by exploiting prior knowledge about the space of RIRs for a given acoustic scenario. The proposed method is based on the projection of the parameter update onto an affine subspace which is selected by a novel computationally efficient computation of the associated evidence. The benefit of the proposed update denoising for a state-of-the-art OSASI algorithm was corroborated by simulated experiments.

Future research aims at evaluating the benefit of various dictionary learning algorithms in comparison to PCA for estimating the model parameters. Furthermore, probabilistic mixtures of subspace models, e.g., [30], are of interest to improve the unsupervised clustering of the training data in Sec. 3. Finally, an adaptive estimation of the noise variances by, e.g., an Expectation-Maximization (EM) framework, and an adaptive computation of the optimum subspace dimension appears to be promising for non-stationary noise signals.

7. REFERENCES

- [1] S. Haykin, *Adaptive filter theory*, Prentice Hall, Upper Saddle River, NJ, 2002.
- [2] P. S. R. Diniz, *Adaptive Filtering: Algorithms and Practical Implementation*, Springer, Berlin, Heidelberg, 2007.
- [3] H. Buchner, J. Benesty, and W. Kellermann, “Generalized multichannel frequency-domain adaptive filtering: efficient realization and application to hands-free speech communication,” *Signal Processing*, vol. 85, no. 3, pp. 549–570, Mar. 2005.
- [4] S. Malik and G. Enzner, “Recursive Bayesian Control of Multichannel Acoustic Echo Cancellation,” *IEEE Signal Processing Letters*, vol. 18, no. 11, pp. 619–622, Nov. 2011.
- [5] T. Gansler, M. Hansson, C.-J. Ivarsson, and G. Salomonsson, “A double-talk detector based on coherence,” *IEEE Transactions on Communications*, vol. 44, no. 11, pp. 1421–1427, Nov. 1996.
- [6] J. Benesty, D.R. Morgan, and J.H. Cho, “A new class of double-talk detectors based on cross-correlation,” *IEEE Transactions on Speech and Audio Processing*, vol. 8, no. 2, pp. 168–172, Mar. 2000.
- [7] S. Malik and G. Enzner, “Online maximum-likelihood learning of time-varying dynamical models in block-frequency-domain,” in *International Conference on Acoustics, Speech and Signal Processing (ICASSP)*, Dallas, USA, Mar. 2010.
- [8] M. Fozunbal, T. Kalker, and R. W. Schafer, “Multi-Channel Echo Control by Model Learning,” in *International Workshop on Acoustic Echo and Noise Control (IWAENC)*, Seattle, USA, Sept. 2008.
- [9] T. Koren, R. Talmon, and I. Cohen, “Supervised system identification based on local PCA models,” in *International Conference on Acoustics, Speech and Signal Processing (ICASSP)*, Kyoto, Japan, Mar. 2012.
- [10] R. Talmon and S. Gannot, “Relative transfer function identification on manifolds for supervised GSC beamformers,” in *European Conference on Signal Processing (EUSIPCO)*, Marrakech, Morocco, Sept. 2013.
- [11] R. Talmon, I. Cohen, S. Gannot, and R. R. Coifman, “Diffusion Maps for Signal Processing: A Deeper Look at Manifold-Learning Techniques Based on Kernels and Graphs,” *IEEE Signal Processing Magazine*, vol. 30, no. 4, pp. 75–86, July 2013.
- [12] B. Laufer-Goldshtein, R. Talmon, and S. Gannot, “A Study on Manifolds of Acoustic Responses,” in *Latent Variable Analysis and Signal Separation (LVA/ICA)*, Liberec, Czech Republic, Aug. 2015.
- [13] L.W. Tu, *An Introduction to Manifolds*, Universitext. Springer New York, 2010.
- [14] M.M. Sondhi, D.R. Morgan, and J.L. Hall, “Stereophonic acoustic echo cancellation—an overview of the fundamental problem,” *IEEE Signal Processing Letters*, vol. 2, no. 8, pp. 148–151, Aug. 1995.
- [15] J. Benesty, D.R. Morgan, and M.M. Sondhi, “A better understanding and an improved solution to the specific problems of stereophonic acoustic echo cancellation,” *IEEE Transactions on Speech and Audio Processing*, vol. 6, no. 2, pp. 156–165, Mar. 1998.
- [16] P. J. Dhrymes, *Matrix Vectorization*, Springer New York, NY, 2000.
- [17] M. Elad, *Sparse and Redundant Representations - From Theory to Applications in Signal and Image Processing*, Springer, New York, NY, 2010.
- [18] S. Lloyd, “Least squares quantization in PCM,” *IEEE Transactions on Information Theory*, vol. 28, no. 2, pp. 129–137, Mar. 1982.
- [19] P.-A. Absil, R. Mahony, and R. Sepulchre, *Optimization Algorithms on Matrix Manifolds*, Princeton University Press, Princeton, NJ, 2008.
- [20] C. M. Bishop, *Pattern Recognition and Machine Learning (Information Science and Statistics)*, Springer, Berlin, Heidelberg, 2007.
- [21] J. Ding, V. Tarokh, and Y. Yang, “Model selection techniques: An overview,” *IEEE Signal Processing Magazine*, vol. 35, no. 6, pp. 16–34, 2018.
- [22] S. Roweis and Z. Ghahramani, “A unifying review of linear Gaussian models,” *Neural computation*, vol. 11, no. 2, pp. 305–345, 1999.
- [23] G. Enzner, H. Buchner, A. Favrot, and F. Kuech, “Acoustic Echo Control,” in *Academic Press Library in Signal Processing*, vol. 4, pp. 807–877. Elsevier, 2014.
- [24] G. Strang, *Linear Algebra and its Applications*, Thomson, Brooks/Cole, Belmont, CA, 2006.
- [25] J. B. Allen and D. A. Berkley, “Image method for efficiently simulating small-room acoustics,” *Journal of the Acoustical Society of America*, vol. 65, no. 4, pp. 943–950, 1979.
- [26] E. Habets, “Room Impulse Response Generator,” Tech. Rep., Technische Universiteit Eindhoven, Sept. 2010.
- [27] D. Arthur and V. Vassilvitskii, “K-means++: The advantages of careful seeding,” in *Proceedings of the 18th Annual ACM-SIAM Symposium on Discrete Algorithms*, New Orleans, USA, 2007.
- [28] L. M. Panfili, J. Haywood, D. R. McCloy, P. E. Souza, and R. A. Wright, “The UW/NU corpus, version 2.0,” <https://depts.washington.edu/phonlab/projects/uwnu.php>, 2017.
- [29] C. Breining, P. Dreiscitel, E. Hansler, A. Mader, B. Nitsch, H. Puder, T. Schertler, G. Schmidt, and J. Tilp, “Acoustic echo control. an application of very-high-order adaptive filters,” *IEEE Signal Processing Magazine*, vol. 16, no. 4, pp. 42–69, 1999.
- [30] M. E Tipping and C. M Bishop, “Mixtures of Probabilistic Principal Component Analysers,” *Neural Computation*, vol. 11, no. 2, pp. 443–482, Feb. 1999.